

9
10
11 **Supp. Figure 1: Cell displacements on thick matrices**
12

- 13 A. Similar to trends observed with $\langle \epsilon_{\phi\phi} \rangle$, $\langle u_{\phi\phi} \rangle$ scales with E_{gel} in a power-law dependent
14 manner, with stem cells being maximally mechanosensitive.
15
16
17 B. Lateral propagation of displacements for a stem cell on gels of different stiffness. The
18 common, characteristic decay length is $\sim 0.25 R_{cell}$.
19
20
21
22
23

24 **Supp. Figure 2: Depth sensing: gel strain distributions**
25

26 Individual interfacial strain components ($\langle \epsilon_{rr} \rangle$, $\langle \epsilon_{zz} \rangle$, $\langle \epsilon_{rz} \rangle$, $\langle \epsilon_{\theta\theta} \rangle$) plotted versus gel thickness
27
28 for different values of E_{gel} exhibit different transition regimes.
29
30
31
32

33 **Supp. Figure 3: Comparison of prestress distributions (soft gel)**
34

35 Uniform prestress distribution, used in this paper is compared with edge prestress and interfacial
36 prestress to study differences in the displacement and strain maps. In comparison to edge
37 prestress, where peak displacements and strain compare well with those obtained with uniform
38 prestress, where peak displacements and strain compare well with those obtained with uniform
39 prestress, interfacial prestress produces very low displacement and strains.
40
41
42
43
44
45
46
47
48
49
50
51
52
53
54
55
56
57
58
59
60
61
62
63
64
65

Figure S1

Shamik Sen

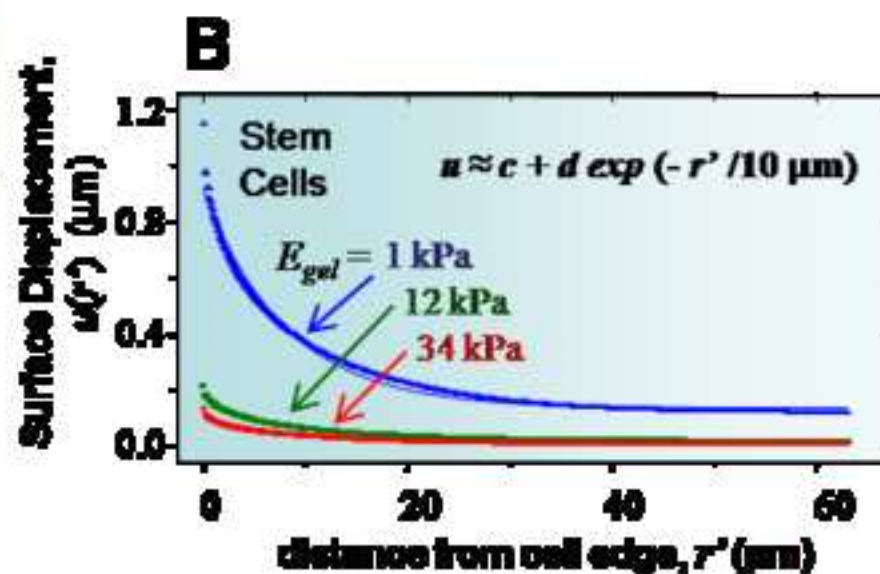
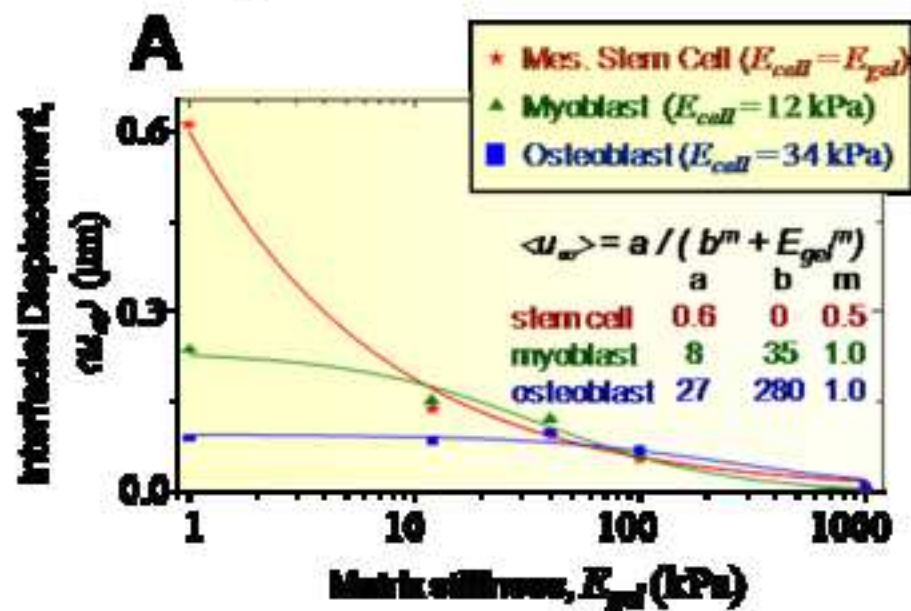


Figure S2

Shamik Sen

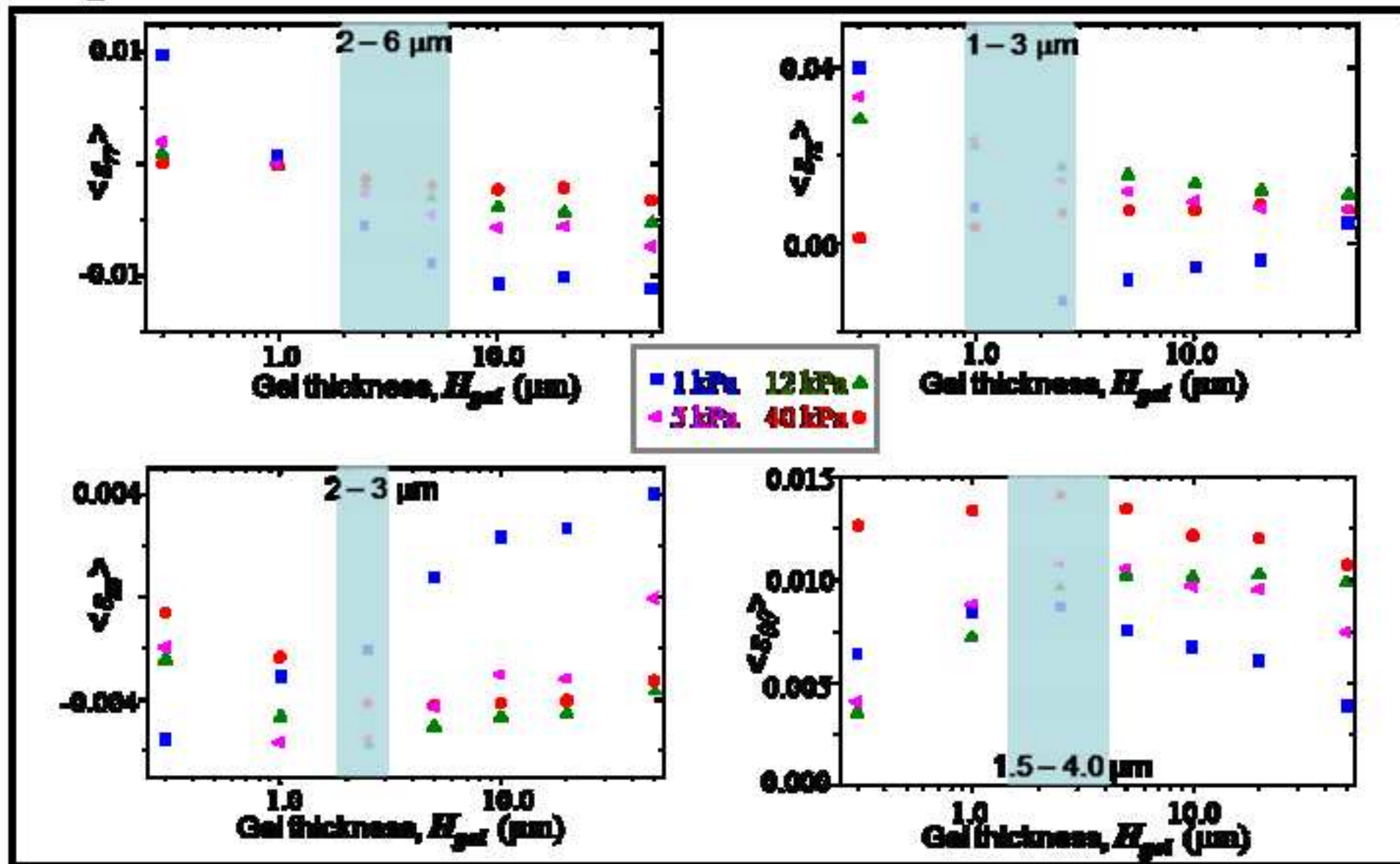
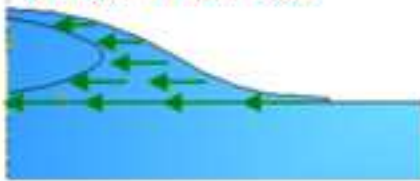


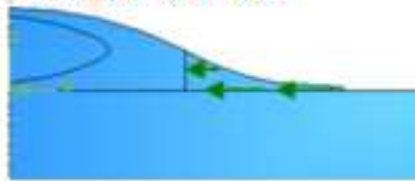
Figure S3

Shamik Sen

Uniform Prestress



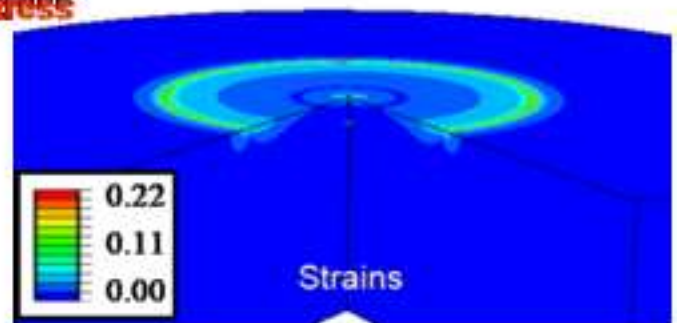
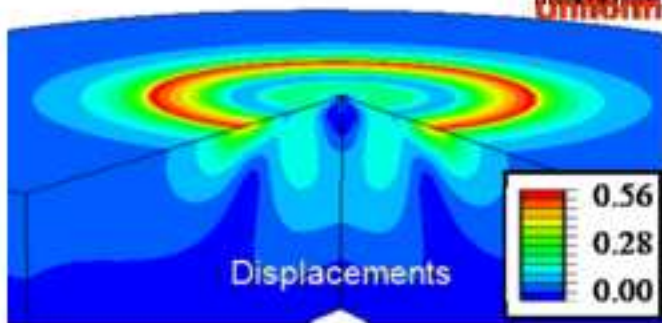
Edge Prestress



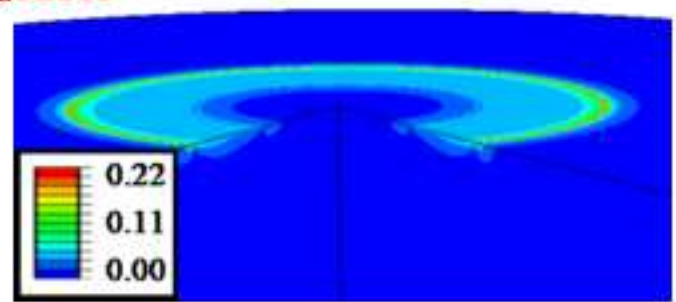
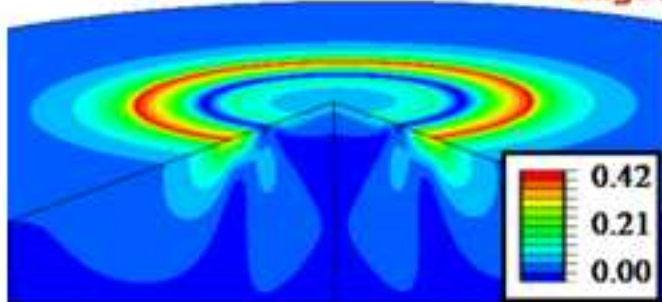
Interfacial Prestress



Uniform Prestress



Edge Prestress



Interfacial Prestress

